ADHESIVES

Tough adhesives for diverse wet surfaces

J. Li,[1,2,3] A. D. Celiz,[2,4]* J. Yang,[1,5]* Q. Yang,[1,5,6] I. Wamala,[7] W. Whyte,[1,2,8] B. R. Seo,[1,2] N. V. Vasilyev,[7] J. J. Vlassak,[1] Z. Suo,[1,5] D. J. Mooney[1,2]†

Adhesion to wet and dynamic surfaces, including biological tissues, is important in many fields but has proven to be extremely challenging. Existing adhesives are cytotoxic, adhere weakly to tissues, or cannot be used in wet environments. We report a bioinspired design for adhesives consisting of two layers: an adhesive surface and a dissipative matrix. The former adheres to the substrate by electrostatic interactions, covalent bonds, and physical interpenetration. The latter amplifies energy dissipation through hysteresis. The two layers synergistically lead to higher adhesion energies on wet surfaces as compared with those of existing adhesives. Adhesion occurs within minutes, independent of blood exposure and compatible with in vivo dynamic movements. This family of adhesives may be useful in many areas of application, including tissue adhesives, wound dressings, and tissue repair.

Adhesives that can bond strongly to biological tissues would have broad applications ranging from tissue repair (*1*, *2*) and drug delivery (*3*, *4*) to wound dressings (*5*, *6*) and biomedical devices (*7*, *8*). However, existing tissue adhesives are far from ideal. Cyanoacrylate (Super Glue) is the strongest class of tissue adhesive (*9*) but is cytotoxic; is incompatible with wet surfaces, as it solidifies immediately upon exposure to water; and forms rigid plastics that cannot accommodate dynamic movements of tissues (*10*). Nanoparticle (*11*) and mussel-inspired adhesives (*12*) adhere weakly to tissues, as their adhesion mainly relies on relatively weak physical interactions, typically leading to low adhesion energies of 1 to 10 J m^{-2}. Commercial adhesives, such as the fibrin glue TISSEEL (Baxter) (*13*) and polyethylene glycol–based adhesives (*14*) like COSEAL (Baxter) and DURASEAL (Confluent Surgical), can form covalent bonds with tissues. However, their matrix toughness and adhesion energies are on the order of 10 J m^{-2} (*15*). Such brittle adhesives are vulnerable to debonding because of cohesive failure in the adhesive matrix. For comparison, cartilage constitutes a matrix of high toughness (1000 J m^{-2}) and bonds to bones with an adhesion energy of 800 J m^{-2} (*16*).

[1]John A. Paulson School of Engineering and Applied Sciences, Harvard University, Cambridge, MA 02138, USA. [2]Wyss Institute for Biologically Inspired Engineering, Harvard University, Cambridge, MA 02138, USA. [3]Department of Mechanical Engineering, McGill University, Montreal, Quebec H3A 0G4, Canada. [4]Advanced Materials and Healthcare Technologies Division, School of Pharmacy, University of Nottingham, Nottingham NG7 2RD, UK. [5]Kavli Institute for Nanobio Science and Technology, Harvard University, Cambridge, MA 02138, USA. [6]School of Aerospace, Tsinghua University, Beijing 100084, People's Republic of China. [7]Departments of Cardiac Surgery, Boston Children's Hospital, Boston, MA 02115, USA. [8]Advanced Materials and Bioengineering Research Centre, Royal College of Surgeons in Ireland and Trinity College Dublin, Dublin, Ireland.
*These authors contributed equally to this work.
†Corresponding author. Email: mooneyd@seas.harvard.edu

Achieving high adhesion energy requires the synergy of two effects. First, the adhesive should form strong bonds with the substrate. Second, materials inside either the adhesive or the substrate (or both) should dissipate energy by hysteresis. Tissue adhesives must also show compatibility with body fluids, as well as with cells and tissues. Here we report the design of a family of tough adhesives (TAs) for biological applications to meet those requirements. The design is inspired by a defensive mucus secreted by slugs (*Arion subfuscus*) that strongly adheres to wet surfaces (*17*). This slug adhesive consists of a tough matrix with interpenetrating positively charged proteins (*18*). Our TAs are made up of two layers: (i) an adhesive surface containing an interpenetrating positively charged polymer and (ii) a dissipative matrix (Fig. 1A). The adhesive surface can bond to the substrate through electrostatic interactions, covalent bonds, and physical interpenetration, whereas the matrix dissipates energy through hysteresis under deformation.

The TAs were designed on the basis of two criteria: (i) The adhesive surface must wet negatively charged surfaces of tissues and cells and must form covalent bonds across the interface while being compliant to the dynamic movements of tissues. (ii) The dissipative matrix must be tough and capable of dissipating energy effectively when the interface is stressed. To satisfy the first criterion, we employed a bridging polymer that bears positively charged primary amine groups under physiological conditions. The primary amine found in the slug adhesive is believed to play a major role in its mechanics and adhesion (*19*). Such a polymer can be absorbed to the tissue surface via electrostatic attractions, enabling primary amine groups to bind covalently with carboxylic acid groups from the hydrogel matrix and the tissue surface (Fig. 1A). If the target surface is permeable, the bridging polymer can also penetrate into the target surface, forming physical entanglements, and chemically anchor the adhesive. The second criterion is satisfied by using a hydrogel capable of dissipating energy as the dissipative matrix. For instance, alginate-polyacrylamide (Alg-PAAm) hydrogels effectively dissipate energy under deformation (*20*). We hypothesize that by combining the interfacial bridging and the background hysteresis, the TAs could form strong adhesion on wet surfaces.

With the use of these design principles, we fabricated a family of TAs that can adhere to wet surfaces. We chose porcine skin as the first model tissue, as it closely resembles human skin and is robust, ensuring that ultimate adhesive failure occurs at the interface. To identify an appropriate bridging polymer, we tested five polymers: chitosan, polyallylamine (PAA), polyethylenimine, collagen, and gelatin. The bridging polymer penetrated rapidly into the hydrogel matrix (fig. S1), forming a positively charged surface (fig. S2). Two coupling reagents, 1-ethyl-3-(3-dimethylaminopropyl)carbodiimide and *N*-hydroxysulfosuccinimide, were applied to facilitate covalent bond formation (*21*, *22*). Other coupling reagents or enzymes, such as transglutaminase, can also enable the formation of interface-bridging covalent bonds (*23*). Our TAs were then applied on the epidermis of porcine skin with compression, and the resulting adhesion was quantified by the adhesion energy (fig. S3) (*24*). Among the tested polymers, PAA and chitosan led to adhesion energies >1000 J m^{-2} (Fig. 1B and fig. S4), probably due to the high concentration of primary amines present on these polymers. In comparison, use of the coupling reagents or the bridging polymer alone yielded adhesion energies of 14 J m^{-2} and 303 J m^{-2}, respectively (fig. S5). Adhesion energy was sensitive to the concentration but not the molecular weight of the bridging polymer (fig. S6).

We next examined the importance of the synergy between interfacial bridging and background hysteresis. Our TAs were compared with adhesives formed with either Alg or PAAm single-network hydrogels, as these do not dissipate energy as effectively as the Alg-PAAm hydrogels (*20*). The coupling reagents and chitosan were again applied for interfacial bridging. The Alg hydrogel led to weak adhesion, as it is vulnerable to rupture and lacks effective energy-dissipating mechanisms to toughen the interface. The PAAm hydrogel resulted in higher adhesion, but not as high as the tough matrix of the Alg-PAAm hydrogel, which enables TAs to integrate high adhesion energy and high matrix toughness simultaneously (Fig. 1C and fig. S4). This specific combination cannot be found among existing tissue adhesives (Fig. 1D and fig. S7), including cyanoacrylate (CA), COSEAL, and a nanoparticle-based adhesive. Commercial adhesives are either formed with a brittle matrix such as COSEAL or lack strong interaction with tissues, as in the case of adhesive bandages (*24*). This finding is also echoed in many studies on adhesion between hard materials and rubbers (*25*, *26*), as well as adhesion between hydrogels and inorganic oxidized surfaces (*27*).

Tough adhesives are applicable to a wide variety of wet surfaces, including tissues and hydrogels.

Our TAs adhered strongly to porcine skin, cartilage, heart, artery, and liver (Fig. 2A). Their adhesion energies on hydrogels are higher than those of the nanoparticle-based adhesives (1 to 10 J m^{-2}) that were recently developed to glue hydrogels (Fig. 2B) (*11*). Unlike tissues, certain hydrogels, such as poly(hydroxyethyl methacrylate), lack the functional groups (amine or carboxylic acid) that we used to form interfacial covalent bonds, but these hydrogels still adhere well to TAs (figs. S8 and S9). Although the bridging polymer was found to interpenetrate into a variety of substrates, the penetration depth in a given time depended on the substrate permeability. Because hydrogels are more permeable than tissues, the penetration depth of fluorescein isothiocyanate–labeled chitosan (FITC-chitosan) in hydrogels was greater than that found in skin or muscle (Fig. 2C and fig. S10) and likely underlies the strong adhesion of TAs to even chemically inert hydrogels.

We next evaluated the capacity of our TAs as tissue adhesives, particularly compared with that of the widely used CA. Our TAs exhibited a rapid increase in adhesion energy to porcine skin over time (Fig. 3A). This rapid but not immediate adhesion is likely to aid clinical translation and adoption of these tissue adhesives, as it allows the material to be applied in a facile manner. In contrast, CA solidifies upon contact with tissues, which makes handling and repositioning difficult (*28*). The formation of tissue adhesion is often complicated in vivo because of exposure to blood and dynamic movements. To simulate this in vitro, the porcine skin was first covered with blood before the application of a TA (fig. S11 and movie S2). The adhesion energy was found to be 1116 J m^{-2}, which indicates strong adhesion even with blood exposure. In contrast, the adhesion provided by CA deteriorates significantly upon exposure to blood (Fig. 3B and fig. S12). Our TAs were further tested on a beating porcine heart in vivo (Fig. 3C). Freshly drawn blood was spread on the heart surface at the site of application, followed by application of a TA and peeling tests (movie S3). A strong adhesion was formed on the dynamic curved surface with a peak strength of 83 ± 31 kPa, which exceeds that of commercially available tissue adhesives (typically ~10 kPa) (*29*). Our TAs were found to maintain strong adhesion (600 J m^{-2}) after being implanted into rats for 2 weeks (fig. S13). They also exhibited excellent biocompatibility: In an in vitro cell study, human dermal fibroblasts were able to maintain full viability after 24-hour culture in a TA-conditioned medium, while the cells cultured in a CA-conditioned medium were unable to spread and exhibited low viability (Fig. 3D and fig. S14). The in vivo biocompatibility of our TAs was evaluated with subcutaneous implantation and myocardium attachment in rats (*24*). After performing a histological assessment, we concluded that the degree of inflammatory reaction produced by our TAs was lower than that produced by CA; additionally, our TAs were comparable to COSEAL in this category (Fig. 3E and fig. S15).

The design of TAs can potentially enable many applications, including the gluing of tissues and attaching devices in vivo, tissue repair, and attaining hemostasis. TAs can readily adhere to liver tissue (Fig. 4A). Tensile testing demonstrated that a TA remained highly stretchable and sustained 14 times its initial length before debonding from the liver. The combination of strong adhesion and large deformability is vital when interfacing tissues and deformable devices, whereas existing adhesives hardly accommodate large deformation. For example, our TAs managed to anchor an actuator, recently developed to support heart function, onto myocardium surfaces (fig. S16). TAs are also potentially useful as a dressing for skin wounds. TAs adhered strongly to the epidermis of mice and readily accommodated dynamic movements of this tissue on the living animal (fig. S17 and movie S4).

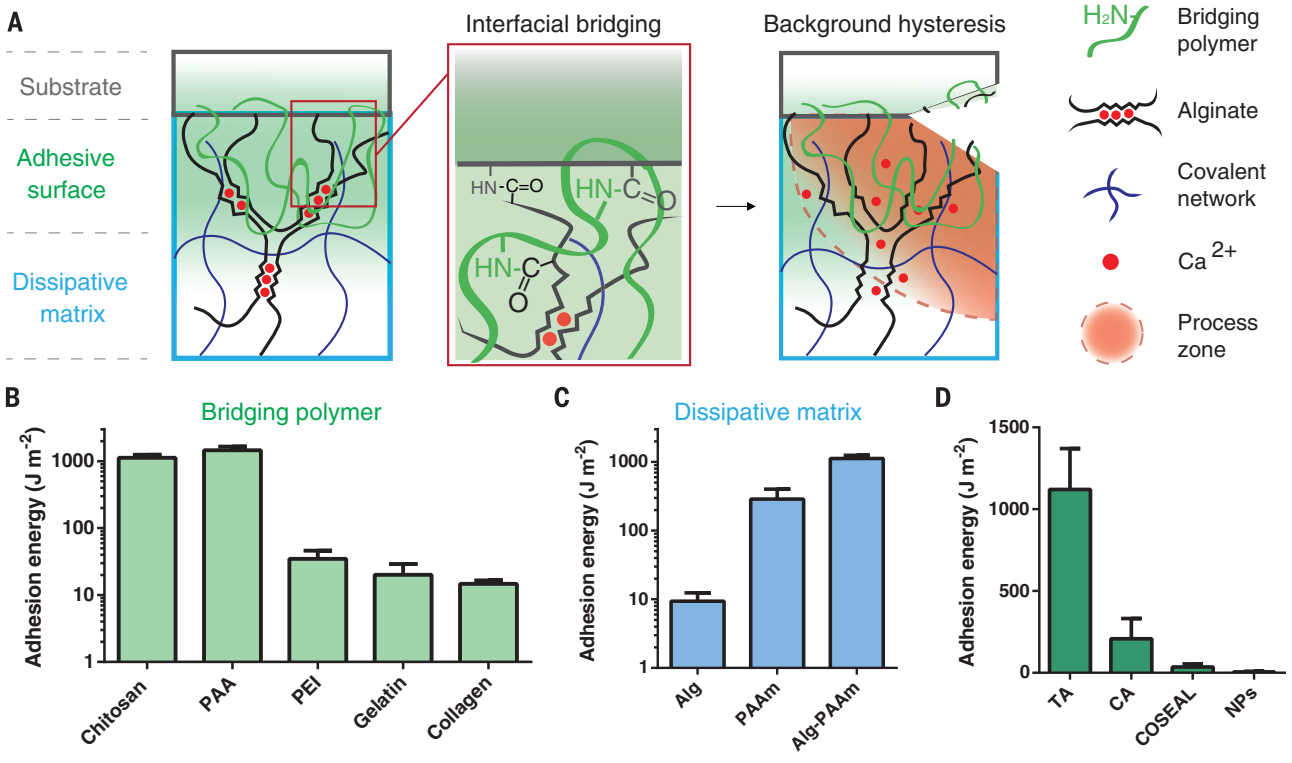

Fig. 1. Design of tough adhesives (TAs). (**A**) TAs consist of a dissipative matrix (light blue square), made of a hydrogel containing both ionically (calcium; red circles) cross-linked and covalently cross-linked polymers (black and blue lines), and an adhesive surface that contains a bridging polymer with primary amines (green lines). The bridging polymer penetrates into the TA and the substrate (light green region). When a crack approaches, a process zone (orange area) dissipates significant amounts of energy as ionic bonds between alginate chains and calcium ions break. (**B**) Adhesion energy on porcine skin was measured using different bridging polymers. PAA, polyallylamine; PEI, polyethylenimine. (**C**) Adhesion energy varies with the hydrogel matrix. Alg, alginate; PAAm, polyacrylamide. (**D**) Comparison between our TAs and other adhesives. CA, cyanoacrylate; NPs, nanoparticles. Error bars indicate SD; *N* = 4 samples.

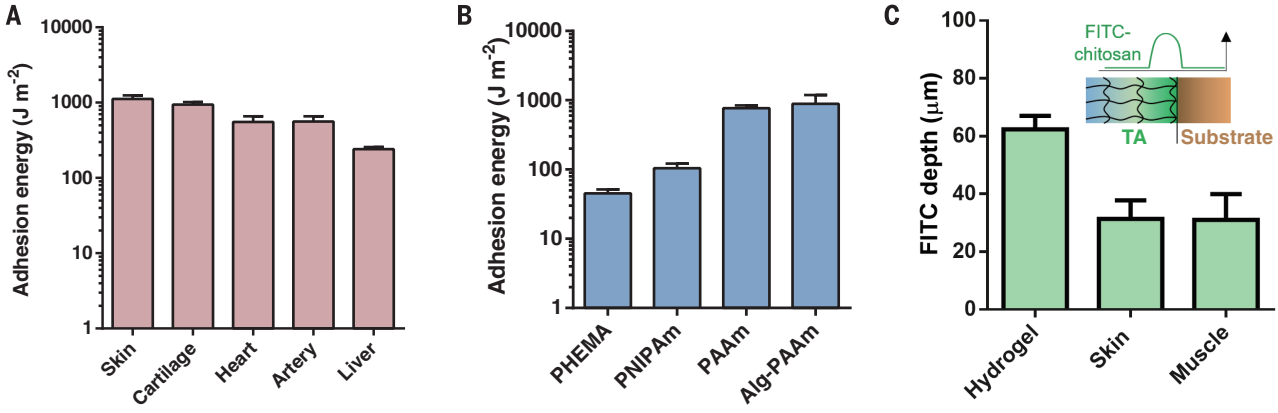

Fig. 2. Adhesion on diverse wet surfaces. TAs adhere to a variety of (**A**) tissue surfaces and (**B**) hydrogels, including poly(hydroxyethyl methacrylate) (PHEMA), poly(*N*′-isopropylacrylamide) (PNIPAm), polyacrylamide (PAAm), and alginate-polyacrylamide (Alg-PAAm) hydrogels. (**C**) Penetration depth of fluorescein isothiocyanate–labeled chitosan (FITC-chitosan) into PAAm hydrogels, skin, and muscle. Error bars indicate SD; *N* = 4.

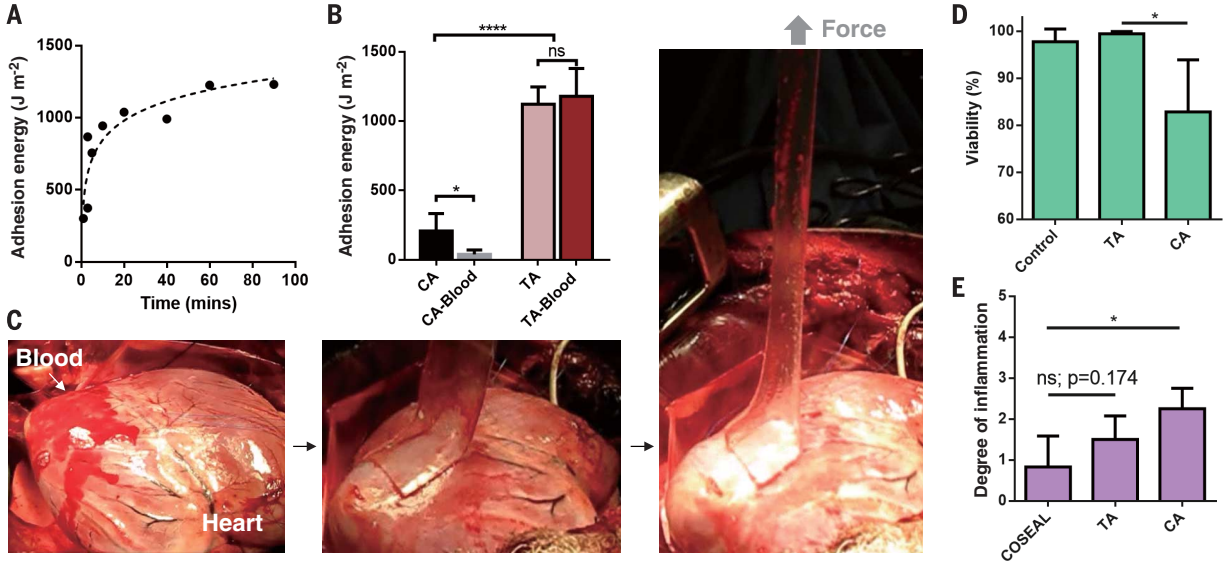

Fig. 3. Adhesion performance and biocompatibility. (**A**) Adhesion kinetics of TAs to porcine skin. (**B**) Comparison of TA versus CA placed on porcine skin with and without exposure to blood. *N* = 4 to 6. (**C**) In vivo test on a beating porcine heart with blood exposure. (**D**) In vitro cell compatibility was compared by quantifying the viability of human dermal fibroblasts. *N* = 4. (**E**) In vivo biocompatibility was evaluated by using subcutaneous implantation in rats. The degree of inflammation was determined by a pathologist (0 = normal, 1 = very mild, 2 = mild, 3 = moderate, 4 = severe, 5 = very severe). Error bars indicate SD; *N* = 4 to 6. *P* values were determined by a Student's *t* test; **P* ≤ 0.05; *****P* ≤ 0.0001; ns, not significant.

A TA can be used for tissue repair as either a preformed patch or an injectable solution. We first tested a TA as a sealant to close a large defect in a porcine heart (Fig. 4B). Our TA was compliant and conformed closely to the geometry of the myocardium. While the heart was being inflated, the sealant expanded with the deformation, and no leakage was observed under strain up to 100%. A perfect seal was maintained after tens of thousands of cycles of inflation-deflation (fig. S18 and movie S5). The measured burst pressures of the TA sealant without and with a plastic backing were 206 mmHg and 367 mmHg, respectively (Fig. 4C); these values exceed normal arterial blood pressure in humans (80 to 120 mmHg) and the performance of commercially available surgical sealants (*24*, *30*). Notably, the TA sealant malfunctioned due to cohesive failure, which is indicative of a strong adhesion interface (fig. S18 and movie S6). We also developed an injectable TA based on an Alg–polyethylene glycol hydrogel (*24*). It can be injected via syringe into a defect site and can form a tough matrix upon exposure to ultraviolet light (fig. S19). As a proof of concept, the injectable TA was used to repair a cylindrical defect in explanted cartilage discs, resulting in recovery of the compressive properties (fig. S20).

Tough adhesives can be used as a hemostatic dressing because of their compatibility with blood exposure, as shown in a hepatic hemorrhage model. A circular laceration was used to produce heavy bleeding on the left lobe of the liver in rats (*24*). Animals were treated immediately with the TA or with a commercial hemostat [SURGIFLO (Ethicon)] as a positive control or were left untreated as a negative control (Fig. 4D). The blood loss was significantly reduced by the application of the TA versus the negative control, and the TA's performance was comparable to that of SURGIFLO (Fig. 4E). All animals survived for the experimental period of 2 weeks without secondary hemorrhage. However, substantial adhesions were found at the lesion site when untreated or treated with SURGIFLO; necrosis occurred in the livers of untreated animals (fig. S21). Neither of these were found in the animals treated with the TA.

We report design principles of biocompatible TAs that combine chemical and physical processes at the interface and in the bulk of the adhesive to

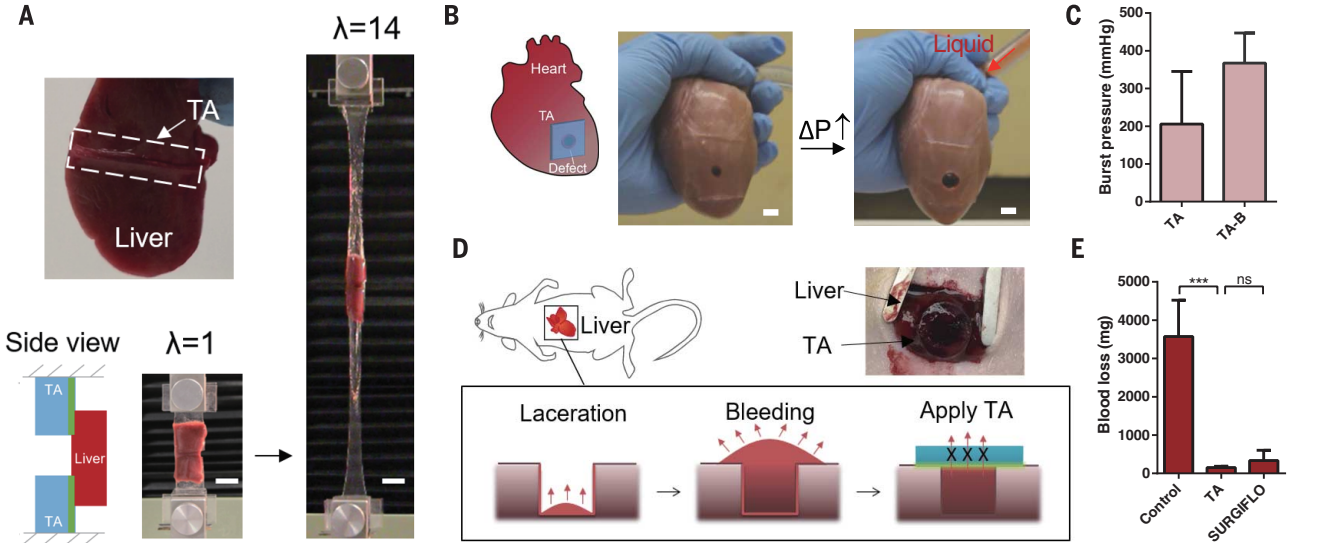

Fig. 4. Application enabled by TAs. (**A**) TAs were used as tissue adhesives. A TA adhered to the liver and sustained 14 times its initial length (λ) before debonding. Scale bars, 20 mm. (**B**) TAs served as heart sealants. The TA sealant prevented liquid (red) leakage as the porcine heart was inflated. ΔP, change in pressure. Scale bars, 10 mm. (**C**) Burst pressures of the TA sealant were measured without (TA) and with plastic backing (TA-B). (**D**) Use of a TA as a hemostatic dressing. A deep wound was created on rat liver and then sealed with a TA to stop the blood flow (labeled with red arrows). (**E**) Blood loss with the treatment of TA, SURGIFLO hemostat, and control (without treatment). Error bars indicate SD; $N = 4$. P values were determined by a Student's t test; $^{***}P \leq 0.001$; ns, not significant.

achieve high adhesion energy on various wet and dynamic surfaces. The mechanical performance and compatibility with cells and tissues allow these materials to meet key requirements for next-generation tissue adhesives.

REFERENCES AND NOTES

1. S. Duflo, S. L. Thibeault, W. Li, X. Z. Shu, G. D. Prestwich, *Tissue Eng.* **12**, 2171–2180 (2006).
2. B. Sharma *et al.*, *Sci. Transl. Med.* **5**, 167ra6 (2013).
3. M. R. Prausnitz, R. Langer, *Nat. Biotechnol.* **26**, 1261–1268 (2008).
4. J. Li, D. J. Mooney, *Nat. Rev. Mater.* **1**, 16071 (2016).
5. C. Ghobril, K. Charoen, E. K. Rodriguez, A. Nazarian, M. W. Grinstaff, *Angew. Chem. Int. Ed.* **52**, 14070–14074 (2013).
6. M. W. Grinstaff, *Biomaterials* **28**, 5205–5214 (2007).
7. E. T. Roche *et al.*, *Adv. Mater.* **26**, 1200–1206 (2014).
8. R. Feiner *et al.*, *Nat. Mater.* **15**, 679–685 (2016).
9. K. A. Vakalopoulos *et al.*, *Ann. Surg.* **261**, 323–331 (2015).
10. H. V. Vinters, K. A. Galil, M. J. Lundie, J. C. Kaufmann, *Neuroradiology* **27**, 279–291 (1985).
11. S. Rose *et al.*, *Nature* **505**, 382–385 (2014).
12. D. G. Barrett, G. G. Bushnell, P. B. Messersmith, *Adv. Healthc. Mater.* **2**, 745–755 (2013).
13. D. H. Sierra, *J. Biomater. Appl.* **7**, 309–352 (1993).
14. D. G. Wallace *et al.*, *J. Biomed. Mater. Res.* **58**, 545–555 (2001).
15. A. K. Dastjerdi, M. Pagano, M. T. Kaartinen, M. D. McKee, F. Barthelat, *Acta Biomater.* **8**, 3349–3359 (2012).
16. M. Moretti *et al.*, *J. Biomech.* **38**, 1846–1854 (2005).
17. J. M. Pawlicki *et al.*, *J. Exp. Biol.* **207**, 1127–1135 (2004).
18. A. M. Wilks, S. R. Rabice, H. S. Garbacz, C. C. Harro, A. M. Smith, *J. Exp. Biol.* **218**, 3128–3137 (2015).
19. M. Braun, M. Menges, F. Opoku, A. M. Smith, *J. Exp. Biol.* **216**, 1475–1483 (2013).
20. J. Y. Sun *et al.*, *Nature* **489**, 133–136 (2012).
21. N. Nakajima, Y. Ikada, *Bioconjug. Chem.* **6**, 123–130 (1995).
22. M. A. Gilles, A. Q. Hudson, C. L. Borders Jr., *Anal. Biochem.* **184**, 244–248 (1990).
23. J. G. Fernandez *et al.*, *Tissue Eng. Part A* **23**, 135–142 (2017).
24. Materials and methods are available as supplementary materials.
25. A. N. Gent, *Langmuir* **12**, 4492–4496 (1996).
26. J. W. Hutchinson, Z. Suo, *Adv. Appl. Mech.* **29**, 63–191 (1992).
27. H. Yuk, T. Zhang, S. Lin, G. A. Parada, X. Zhao, *Nat. Mater.* **15**, 190–196 (2016).
28. T. Stefanov, B. Ryan, A. Ivanković, N. Murphy, *Int. J. Adhes. Adhes.* **68**, 142–155 (2016).
29. N. Lang *et al.*, *Sci. Transl. Med.* **6**, 218ra6 (2014).
30. P. K. Campbell, S. L. Bennett, A. Driscoll, A. S. Sawhney, "Evaluation of absorbable surgical sealants: In vitro testing" (Covidien, 2005); www.covidien.com/imageServer.aspx/doc179399.pdf?contentID=14109&contenttype=application/pdf.

ACKNOWLEDGMENTS

This work was supported by the NIH under award R01DE0130333 and was performed, in part, at the Center for Nanoscale Systems at Harvard University. A.D.C. acknowledges support from a Marie Curie International Outgoing Fellowship funded by the European Commission (agreement 629320). W.W. acknowledges support from Science Foundation Ireland under grant SFI/12/RC/2278. Q.Y. acknowledges a scholarship from Tsinghua University. Z.S. and J.J.V. acknowledge support from the NSF under award CMMI-1404653. Z.S., J.J.V., and D.J.M. acknowledge support from the Harvard University Materials Research Science and Engineering Center (grant DMR-1420570). J.L., A.D.C., and D.J.M. are inventors on U.S. patent applications (US 62/311,646, US 62/356,939, and PCT/US2017/023538) submitted by Harvard University that cover the design of TAs.

SUPPLEMENTARY MATERIALS

www.sciencemag.org/content/357/6349/378/suppl/DC1
Materials and Methods
Supplementary Text
Figs. S1 to S21
References (*31*–*49*)
Movies S1 to S6

25 July 2016; resubmitted 27 April 2017
Accepted 22 June 2017
10.1126/science.aah6362

Tough adhesives for diverse wet surfaces

J. Li, A. D. Celiz, J. Yang, Q. Yang, I. Wamala, W. Whyte, B. R. Seo, N. V. Vasilyev, J. J. Vlassak, Z. Suo and D. J. Mooney

Science **357** (6349), 378-381.
DOI: 10.1126/science.aah6362

Sticky even when wet

Tissue adhesives are used as an alternative to stitches or staples and can be less damaging to the healthy tissues. But they can suffer from low biocompatibility and poor matching of the mechanical properties with the tissues. Li *et al.* combined an adhesive surface with a flexible matrix to develop an adhesive that has the right level of stick but moves with the surrounding tissues. The adhesive is effective in the presence of blood and thus might work during wound repair.

Science, this issue p. 378